10-25 NM PIEZOELECTRIC NANO-ACTUATORS AND NEMS SWITCHES FOR MILLIVOLT COMPUTATIONAL LOGIC

Usama Zaghloul and Gianluca Piazza
Electrical and Computer Engineering Department, Carnegie Mellon University, Pittsburgh, Pennsylvania, USA

ABSTRACT

This paper reports, for the first time, on the design, fabrication, and measurement of piezoelectric nano-actuators and novel stress-compensating NEMS switches based on 10-25 nm thick aluminum nitride (AlN) films. These ultrathin, highly *c*-axis oriented, and low-stress AlN films were synthesized over very thin platinum layers using reactive sputtering. The extracted d_{31} piezoelectric coefficients are -1.73 pC/N and -1.77 pC/N for the 10 nm and 25 nm films, respectively (90% and 92% of their microscale counterpart). Thanks to the scaling of the piezoelectric film thickness and the proposed switch design, the switch exhibits a threshold voltage of 0.2 mV and a subthreshold slope of 0.033 mV/decade –the smallest ever reported for a mechanical transistor. Overall, the NEM relay exhibits a switching energy of ~ 0.01 aJ, making it a very promising candidate for ultralow power digital computing and memory applications.

INTRODUCTION

Significant advances in MEMS technologies in recent decades lead to reconsidering mechanical logic, which historically was conceived much earlier than its electronic alternative [1]. This is supported by the fundamental physical limitations that hinder further scaling of metal-oxide-semiconductor (MOS) transistors attributed mainly to the subthreshold leakage. NEMS switches were proposed as very promising alternative to resolve this constraint, and were demonstrated to implement digital logic [2, 3] and memories [4]. Replacing the semiconductor channel between the source and drain in MOS transistors by an air gap in NEMS switches results in a much steeper subthreshold slope. NEMS switches are also well suited for harsh environments due to their radiation and temperature tolerance [5].

While there are different actuation mechanisms for NEMS devices, the most used for switches are electrostatic [2] and piezoelectric [3, 6] methods, with piezoelectric switches exhibiting linear actuation and lower power consumption. Further miniaturization of NEMS switches will lead to more reduced switching energy, smaller footprint, and faster switching. There are two main bottlenecks for the scaling of piezoelectric NEMS switches: (i) synthesis of ultrathin highly oriented and low stress piezoelectric films, and (ii) fabricating and maintaining nanometer height switching gaps after releasing the device.

This paper addresses these bottlenecks and reports piezoelectric nano-actuators and NEMS switches based on ultrathin (10-25 nm) highly *c*-axis oriented and low stress AlN films synthesized on well-textured ultrathin Pt layers (2-10 nm). Moreover, a novel stress-compensating switch geometry was proposed and characterized to realize nanometer height switching gaps.

DESIGN OF ACTUATORS AND SWITCHES

Piezoelectric nano-actuators

Two different types of piezoelectric unimorph actuators were designed and fabricated. The first type consists of a three-layer stack (Fig. 1a) where the piezoelectric AlN film is sandwiched between two metal electrodes, each consists of Ti/Pt layers, with the thicker metal electrode (the elastic layer) deposited on top of the AlN film to enhance the step coverage of the AlN over a thinner bottom electrode, hence improving the yield. The second unimorph actuator is a four-layer stack (Fig. 1b) where the elastic layer is composed of two layers; an AlN seed layer and the bottom electrode. The four-layer actuator is used to reduce the substrate leakage, to enable using thinner bottom metal layers to improve the step coverage, and finally to study the impact of the AlN seed layer on the orientation of the piezoelectric film.

For unimorph actuators, the thickness of the elastic layer can be optimized to obtain maximum electromechanical coupling coefficient, hence maximum displacement. Also, for nano-actuators, the thickness of the electrode layer bonded to the other side of the piezoelectric AlN film (over or under the piezoelectric layer in the four- or three-layer actuators, respectively) is comparable to the thickness of the scaled piezoelectric film, and consequently its impact cannot be ignored. Therefore, for both types of actuators investigated in this work, the thicknesses of the elastic layers and the metal electrodes were optimized using a complex analytical model that considers all layers in the stack [7]. This model was also verified by finite element analysis (FEA) using COMSOL as shown in Fig. 1c. The influence of the top and bottom Pt layers and the agreement between the analytical and FEA data are obvious from the figure.

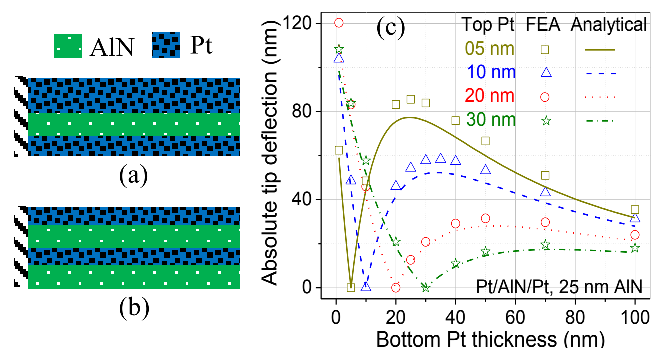

Figure 1. Design of piezoelectric nano-actuators: The layer structure of (a) three-layer, and (b) four-layer unimorph actuators; (c) thickness optimization of the elastic/electrode layers.

Triple beam NEMS switches

A key challenge that stands against further miniaturization of NEMS switches is the synthesis of few nanometers height switching gaps in released devices due

to the residual stresses in the movable parts. This is also harder to control in piezoelectric switches considering the multilayer structure of the actuators and the tiny thickness of each layer forming them. Beyond directly addressing the issue of residual stress during the deposition of each constituting layer, we also demonstrated a novel stress-compensating NEMS switch design (Fig. 2). The switch has four terminals: source, drain, gate, and body, and consists of three curved and suspended beams placed next to each other. The center beam carries the nano-actuator and the tip (the top contacting metal) in the longitudinal direction of the beams, while the two outer symmetric beams are clamped at their free-ends and carry the source and drain bottom contacting metals in the transverse direction. The potential applied to the piezoelectric actuator (between the gate and the body) is used to create or remove a conducting channel between the drain and source through the tip.

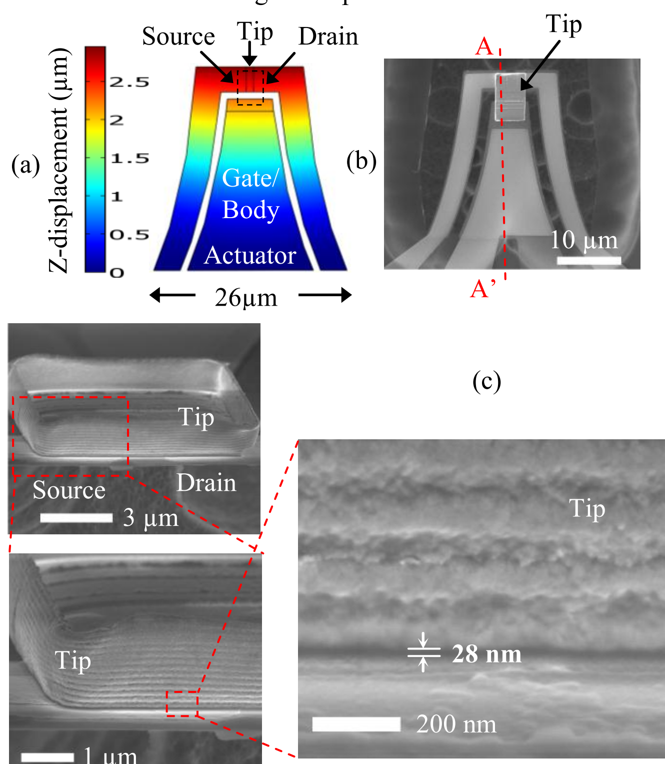

Figure 2. Triple beam NEMS switch: (a) FEA showing the device terminals, and (b, c) SEM images of a finished device.

Such design resembles a differential topology since the stress gradient of the center beam is an average of the stresses of the outer beams. Consequently, the stress-induced deflection of the center beam will be an average of the deflections of the outer beams independently of the stress gradient distributions in the three beams, hence maintaining the nanometer gap height. Figs. 2b and c show SEM images of a finished NEMS switch and its contact area, respectively. Thanks to the differential topology of the triple beam design, a 28 nm air gap was maintained after etching the sacrificial layer, despite an overall residual stress gradient present in the thin film stack. Using curved beams in the proposed switch has an important advantage over rectangular ones since the former averages the in-plane stresses in x-y directions between the center and outer beams across the whole beams' length. This in turn reduces the displacement difference due to any asymmetry in the in-plane stresses in the three beams. Moreover, the use of actuator with a larger width at the anchor location results in higher flexural rigidity of the center beam, hence larger restoring forces, which facilitates overcoming the surface forces when opening the switch. Finally, the thickness of the elastic layers of the nano-actuators used to realize the switch was optimized using FEA to produce maximum contact force.

SYNTHESIS OF ULTRATHIN ALN FILMS

Well-textured ultrathin Pt layers (2-10 nm) were synthesized on very thin titanium (Ti) films (0.5-2 nm), both using dc sputtering on 100-mm diameter (100) Si wafers. We found that the argon (Ar) pressure used during the Pt sputtering has a considerable effect on the crystal orientation of the subsequently deposited AlN film and typically on the residual stress of the Pt film. Smaller Ar pressure (~21 mTorr) was found to be optimal for enhanced AlN crystal orientation and adequate residual stress in the Pt films (±75 Mpa).

The AlN films were deposited by AC reactive sputtering from 99.999% Al target using Tegal AMS SMT system with the dual cathode S-Gun magnetron source. Before depositing the AlN film, a preliminary substrate etching is performed to prepare the surface for better AlN nucleation. We developed two recipes for both the substrate etching and the AlN sputtering. We found that a reduced rf power (~30W) and a shorter etching duration (~40 seconds) are optimal for the substrate pre-etching to avoid complete removal of the Ti/Pt layers and obtain a well-oriented AlN film. During the AlN sputtering process, a process work point on the hysteresis curve of the magnetron discharge is controlled by the partial pressures of nitrogen (N_2) and Ar as determined by the gas flows. A three-step recipe for the reactive sputtering process was developed to provide better conditions for AlN nucleation on the ultrathin Pt surface. Each step has a different process work point on the hysteresis curve, where the first step is controlled to be in the deeper poison mode, the second step in the poison mode center, and the third step in the poison mode at the work point closer to the transition area between poison and metallic modes [8]. In addition to adjusting the N_2 and Ar flows to maintain these process working points, the Ar flow was optimized to reduce in-plane stress and the stress gradient in the AlN films. The full width at half maximum (FWHM) of x-ray diffraction (XRD) rocking curve measurements around the diffraction peak AlN (0002) was used to characterize the film quality (smaller FWHM means better crystal orientation). The 25 nm and 10 nm thick AlN films synthesized in this study exhibit FWHM of 4.1° and 4.7°, respectively.

FABRICATION PROCESS

The nano-actuators and switches were fabricated using four and seven photolithography masks, respectively (Fig. 3). First, an AlN insulation layer was deposited on high resistivity Si substrate for the four-layer actuator by reactive sputtering followed by patterning the bottom Pt electrode by lift-off. Next, highly *c*-axis oriented and low stress piezoelectric AlN film was deposited by reactive

sputtering over the Pt layer using the two developed recipes. Then, vias were formed in the piezoelectric AlN film using hot phosphoric acid at 150°C to access the bottom electrode (Fig. 3a). This is followed by patterning the top Pt layer using Lift-off to define the actuator's top electrode and the bottom contacting metal of the switch. The lateral dimensions of the actuators were then defined by dry etching the AlN using $Cl_2/BCl_3/Ar$ chemistry (Fig. 3b). Next, an ultrathin sacrificial layer of amorphous Si (~30 nm) was deposited and patterned by lift-off to define the switch air gap followed by patterning the top Pt contacting metal (the Tip) by lift-off. A photoresist mask was used then to define small openings around the switch contact area (Fig. 3c), and the sacrificial layer and the Si were etched by XeF_2 to release the devices. The photoresist was then etched using consecutive steps of plasma ashing and descumming (Fig. 3d).

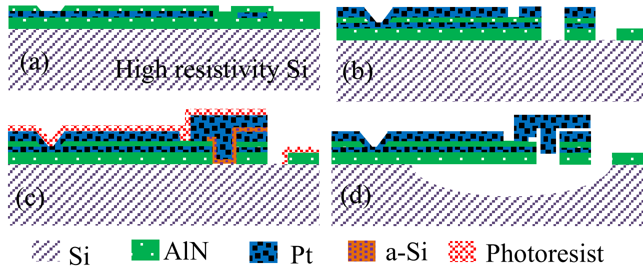

Figure 3. Fabrication process flow for the actuators and switches described at the cross section A-A' shown in Fig 2b.

RESULTS AND DISCUSSION

Piezoelectric nano-actuators

The deflection profiles for a three-layer actuator with 10 nm thick AlN film (actuator A) under different applied bias were measured using an optical profilometer (Fig. 4a). This unimorph, which is the thinnest ever reported piezoelectric actuator to our knowledge, has a giant tip deflection of ~1.1 µm for an applied bias of only 0.7 V thanks to the scaling of the AlN film thickness and the optimization of the elastic/electrode layer thicknesses. The maximum extracted deflection at the actuator tip for actuator A and another four-layer actuator that uses 25 nm thick piezoelectric AlN layer (actuator B) along with the corresponding FEA and analytical results are plotted in Fig 4b. For both actuators, the figure highlights the linear displacement as a function of the applied voltage as well as the symmetry of the actuator response for positive and negative bias. The excellent agreement between the FEA and the analytical data is also obvious from the figure.

The d_{31} piezoelectric coefficients were extracted by fitting the measured actuator deflection to the FEA and analytical data. The d_{31} for the AlN films in actuators A and B are -1.66 pC/N and -1.76 pC/N, respectively (90% and 92%, respectively, of the literature reported values of much thicker AlN films sputtered over much thicker metal layers) [9]. These results agree also with the FWHM values (see inset of Fig. 4b) that show a relative degradation in the film orientation when reducing the thickness from 25 nm to 10 nm. We found that the AlN films implemented in the four-layer actuators exhibit slightly higher d_{31} values than the films realized in the three-layer actuators. This difference, though small, was also confirmed by a relatively smaller difference in FWHM of ~0.18° (better crystal orientation) for the AlN films deposited on (Pt/Ti/AlN seed layer/Si) compared to AlN deposited on (Pt/Ti/Si), and can be attributed to the coherent heteroepitaxial nucleation [10].

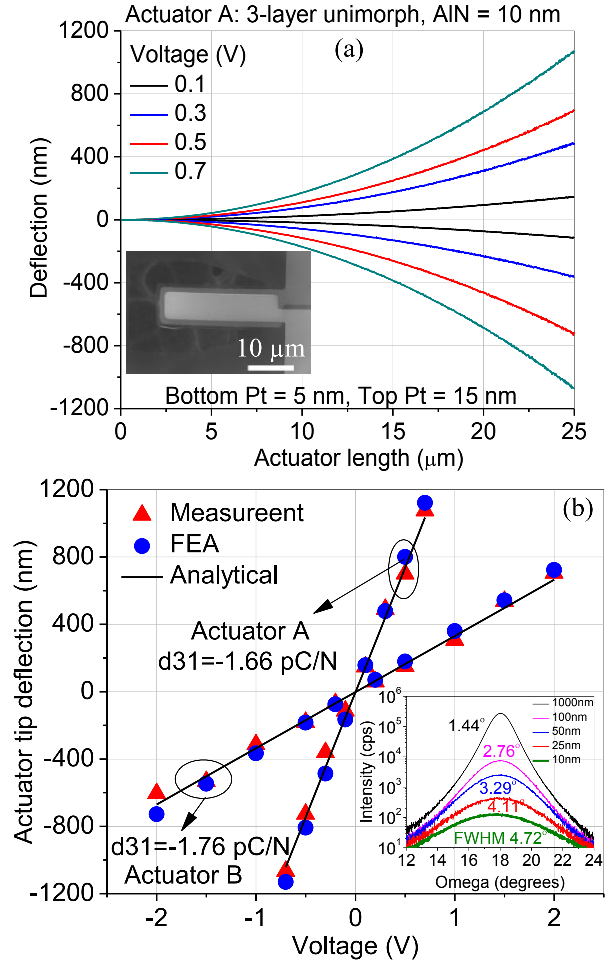

Figure 4. (a) Deflection profile of a three-layer actuator with 10 nm thick AlN piezoelectric film under different voltage, (b) excellent agreement between the experimental, analytical, and FEA results.

Triple beam NEMS switches

The I-V characteristics of the fabricated NEMS switches measured using the body-biasing method [3] is presented in Fig. 5a. This particular switch has a four-layer unimorph actuator with 25 nm thick piezoelectric AlN film, an air gap of around 28 nm (see Fig. 2c), and a footprint of 27 µm x 36 µm (see Fig. 2b). Thanks to the scaling down of the AlN film thickness and to the stress-compensating triple beam design, the switch has a small actuation voltage of only 1.63 V. Moreover, using the body-biasing actuation, V_{th} can be controlled and reduced to 0.2 mV – the smallest ever reported for a mechanical transistor. This extremely small V_{th} along with the high I_{on}/I_{off} switching ratio of ~10^6 result in a subthreshold slope of 0.033 mV/decade, three orders of magnitude smaller than what is achieved by the most mature MOS technology to date. In addition, the relatively scaled actuator's footprint and the very small V_{th} lead to a greatly reduced switching energy ~0.01 aJ that can be practically achieved at the circuit level if methods to set and control the voltages accurately become available. The measured V_{th} under

different applied body bias (V_B) is shown in Fig. 5b and it emphasizes the extreme linearity of the device actuation that has a crucial importance in implementing active pull-off NEMS switches. Though the measured I_{off} of the switch is ~2-3 pA, which is the noise floor of the instrument, we believe that I_{off} is ideally zero due to the presence of the air gap. Finally, the measured contact resistance of the switch is 5.14 KΩ versus a modeled resistance of 10 KΩ.

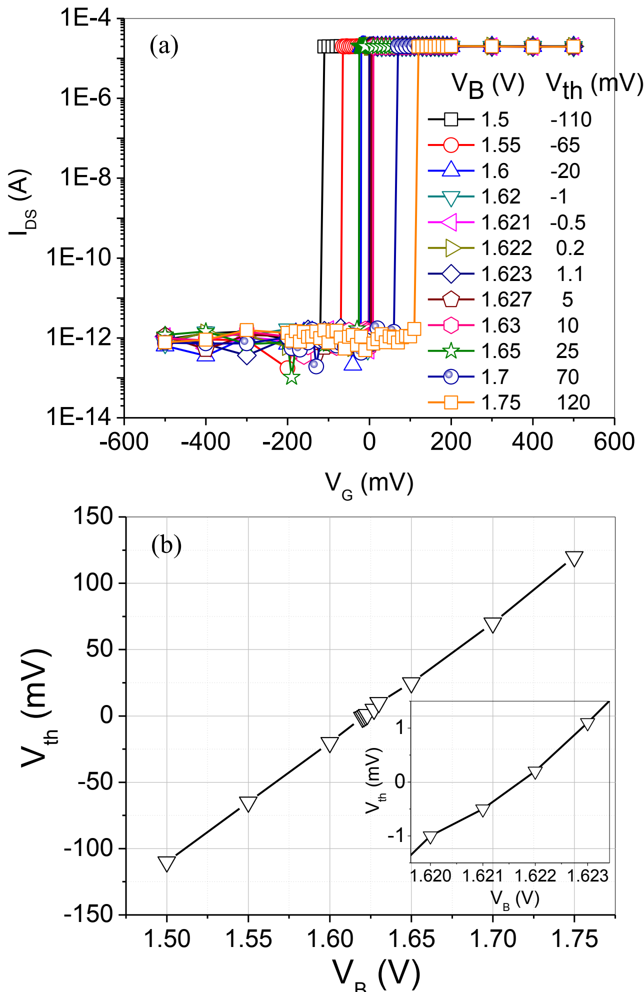

Figure 5. (a) The I-V measurements for a NEMS switch using the body-biasing method. (b) V_{th} versus the body-bias (V_B) highlighting the device linearity.

The active area of the demonstrated NEMS switch is ~187 μm^2 (excluding the connecting traces and contact pads) which is clearly much larger than the active area of state-of-the-art 22 nm MOS technology. However, this piezoelectric switch which is based on 25 nm AlN film has two, three, and eight orders of magnitude smaller device footprint, threshold voltage, and switching energy, respectively, than the recently reported NEMS switches realized using 250 nm thick AlN films [3]. This emphasizes that further scaling of this technology is possible and potentially much smaller devices could be realized in the future. Our scaling analysis shows that the device footprint and the actuation voltage can be further reduced to 2 μm^2 and 0.4 V, respectively, when 10 nm AlN films are used. With future progress in technological solutions to synthesis even thinner AlN films (beyond 1 nm), the analysis highlights that the footprint and voltage can be reduced to 0.023 μm^2 and 90 mV, respectively.

CONCLUSION

We succeeded in the synthesis of the thinnest piezoelectric AlN films (10-25 nm) over ultrathin Pt electrodes (2-10 nm) reported to date. The quality of the grown films was characterized by realizing different types of piezoelectric nano-actuators and novel stress-compensating NEMS switches. The extracted piezoelectric coefficients for the grown ultrathin AlN films have comparable values to their microscale counterpart while the fabricated switches exhibit the smallest ever reported subthreshold slope. The present study creates a pathway toward all mechanical computing with ultra-small energy consumption.

ACKNOWLEDGEMENTS

This work was supported by the DARPA NEMS program. We thank the staff of the Wolf Nanofabrication Facility at the University of Pennsylvania.

REFERENCES

[1] V. Pott, H. Kam, R. Nathanael, J. Jeon, E. Alon, T. J. K. Liu, "Mechanical computing redux: relays for integrated circuit applications", *Proc. of the IEEE*, vol. 98, pp. 2076-2094, 2010.

[2] J. Jeon, V. Pott, H. Kam, R. Nathanael, E. Alon, T. J. K. Liu, "Perfectly complementary relay design for digital logic applications", *IEEE Electron Device Letters*, vol. 31, pp. 371–373, 2010.

[3] N. Sinha, T. Jones, Z. Guo, G. Piazza, "Body-Biased Complementary Logic Implemented Using AlN Piezoelectric MEMS Switches", *J. Microelectromech. Syst.*, vol. 21, pp. 484–496, 2012.

[4] K. Akarvardar, H. Wong, "Ultralow voltage crossbar nonvolatile memory based on energy-reversible NEM switches", *IEEE Electron Device Letters*, vol. 30, pp. 626–628, 2009.

[5] T. Lee, S. Bhunia, M. Mehregany, "Electromechanical Computing at 500°C with Silicon Carbide", *Science*, vol. 329, pp. 1316–1318, 2010.

[6] R. Proie, R. Polcawich, J. Pulskamp, T. Ivanov, M. Zaghloul, "Development of a PZT MEMS switch architecture for low-power digital applications", *J. of Microelectromech. Sys.*, vol. 20, pp. 1032–1042, 2011.

[7] D. DeVoe, A. Pisano, "Modeling and optimal design of piezoelectric cantilever microactuators", *J. of Microelectromech. Syst.*, vol. 6, 266-270, 1997.

[8] V. Felmetsger, P. Laptev, R. Graham, "Deposition of ultrathin AlN films for high frequency electroacoustic devices", *J. of Vac. Sci. & Technology A*, vol. 29, Art. # 021014, 2011.

[9] R. Mahameed, N. Sinha, M. Pisani, G. Piazza, "Dual-beam actuation of piezoelectric AlN RF MEMS switches monolithically integrated with AlN contour-mode resonators", *J. of Micromechanics and Microengineering*, vol. 18, Art. # 105011, 2008.

[10] T. Kamohara, M. Akiyama, N. Ueno, K. Nonaka, N. Kuwano, "Local epitaxial growth of aluminum nitride and molybdenum thin films in fiber texture using aluminum nitride interlayer", *Applied physics letters*, vol. 89, At. # 071919, 2006.

CONTACT

* G. Piazza: piazza@ece.cmu.edu, U. Zaghloul: uzheiba@andrew.cmu.edu